Supplementary Materials

Supplementary Results

Age Differences in Mean Connectivity Strength

We calculated mean (positive) connectivity strength by averaging links between any two regions. A mixed-model Group×Time ANOVA on mean connectivity during rest, across all three time points, yielded no significant effects (Group: $F_{1,36}$=0.45, p=.508, η_p^2=0.01; other effects *p*s>0.3), suggesting no age or time differences in connectivity strength at rest. Importantly, stronger connectivity for younger than older adults emerged only with shifting from rest to task performance and this difference was alleviated with training. Indeed, a Group×Time×Mode ANOVA on estimates of mean connectivity pre- vs. post-training (Time2 vs. Time3) showed greater overall connectivity in younger than older adults (Group: $F_{1,36}$=5.94, p=0.02, η_p^2=0.14) and a significant Group×Time×Mode interaction ($F_{1,36}$=8.15, p=0.007, η_p^2=0.19), and follow-up *t*-tests showed stronger task-mode connectivity for younger than older adults before (t_{36}=4.15, p<0.001) but not after training (t_{36}=0.52, p=0.608). In addition, a similar pre- vs. post-training Group×Time×Load ANOVA on mean connectivity, across loads common for both groups (i.e., loads 5-8), showed greater overall connectivity for younger compared to older adults (Group: $F_{1,36}$=10.43, p<0.001, η_p^2=0.23) and greater overall connectivity with training (Time: $F_{1,36}$=5.13, p=0.03, η_p^2=0.13).

Within-group Effects of Task-Exposure and Training

We assessed *task-exposure* (Time1 vs. Time2) and *training* effects (Time2 vs. Time3) separately within each group, using Time×Load ANOVAs across group-specific loads (i.e., loads 4-8 in older and loads 5-9 in younger adults) and targeting effects of Time. For older adults, there were no task-exposure or training effects on modularity (*p*s>0.2). In contrast, while younger

adults showed no task-exposure effects on modularity (ps>0.3), they showed greater modularity post- compared to pre-training (Time: $F_{1,19}$=25.88, p<0.001, η_p^2=0.58). These results are in line with effects reported in the main text and suggest that training increases brain-wide modularity specifically in younger adults.

Exposure and Training Effects on Intrinsic Network Segregation

We performed an ancillary analysis examining the effects of age and exposure/training on network segregation (Chan et al., 2014; Wig, 2017), using the Power et al. (2011) intrinsic networks. Network segregation was defined as the difference between within- and between-networks connectivity expressed as a proportion of within-network connectivity [i.e., *Segregation* = $(\bar{Z}_w - \bar{Z}_b)/\bar{Z}_w$, where $\bar{Z}_w$ is the within-networks connectivity and $\bar{Z}_b$ is the between-networks connectivity]. Because the Power et al. node-module affiliations were derived based on young adult and resting-state data, we expected overall similar but potentially less specific effects, due to ignoring age and task-related changes in network topology (see main text). Indeed, we identified lower network segregation for older than younger adults across all time points, for both the rest/task shift (Group: $F_{1,36}$=28.81, p<0.001, η_p^2=0.45) and across WM loads common to both groups (i.e., loads 5-8) (Group: $F_{1,36}$=28.87, p<0.001, η_p^2=0.45), as well as greater segregation decrement with shifting from rest to task mode in older compared to younger adults (Group×Mode: $F_{1,36}$=8.75, p=0.005, η_p^2=0.2) (see Fig. S2-a,b). Critically, we confirmed a Group×Time interaction with training (i.e., Time2 vs. Time3) (Group×Time: $F_{1,36}$=5.63, p=0.023, η_p^2=0.14), indicating more segregated networks with training in younger than older adults. Finally, within groups and across group-specific loads (i.e., loads 5-9 in younger adults and 4-8 in older adults), younger adults showed a trend for greater segregation with training (Time: $F_{1,19}$=3.13, p=0.093, η_p^2=0.14), whereas older adults showed a trend for lower segregation with

training (Time: $F_{1,17}$=4.39, p=0.052, η_p^2=0.21). We posit that using the canonical resting-state community structure for analyses of task-related connectivity is not ideal because it does not account for potential differences in community structure between rest and task. (A similar case can be made for analyses comparing older vs. younger participants because the canonical networks are typically derived based on younger adult data and the community structure may differ between younger and older adults; see Discussion in the main text.) Indeed, when we calculate segregation using the data-driven community structure detected for each individual condition within groups (see Fig. S2-c), younger adults show increased segregation with training (Time: $F_{1,19}$=8.59, p=0.009, η_p^2=0.31) whereas older adults do not (Time: $F_{1,17}$=2.21, p=0.156, η_p^2=0.12), consistent with our modularity results. For these reasons, we contend that modularity is the preferable metric for comparing brain network integration/segregation balance across conditions, particularly when differences in community structure might occur.

Robustness Analyses

Modularity Calculations. First, based on evidence that gamma (γ) values in the range from 1 to 2 are adequate for comparing community structure in younger and older adults (Hughes et al., 2020), we ran the Louvain algorithm over this range in increments of 0.1, and the results were overall consistent (see Fig. S3 and Table S1). Then, we assessed distances between our group-level communities and the Power et al. (2011) canonical networks, using variation of information (Meilă, 2007). (For this step, we sampled the threshold density range in increments of 10%, for computational efficiency.) In addition, we calculated the number of modules and the number of singletons in each network, using a cutoff of N=4 nodes to distinguish between biologically meaningful subnetworks and “orphan” fragments or singletons. We focused primarily on the community structure in younger adults during resting-state because the Power et al. node-module

affiliations were determined based on similar data. For $\gamma = 1.3$, younger adults showed (1) low distance from the Power et al. canonical networks, while (2) the number of modules was equal between younger and older adults (i.e., 5 modules for each) and (3) the number of singletons was low (i.e., ≤2 singletons) (see Fig. S4).

Finally, to ensure that results were not due to a specific brain parcellation, we repeated the analysis using a different atlas, and the results were again similar. We employed the brain atlas by Schaefer et al. (2018), which was generated based on resting-state data from a large participant sample (N = 1,489), using a gradient-weighted Markov Random Field model. To enable comparability with our main analysis, we employed the 300 ROIs version of the atlas. We fitted 5 mm-radius spheres around the centroids of each of the Schaefer et al. ROIs and similarly retained only regions showing >70% mean signal intensity (265 ROIs). We used the same processing pipeline and parameters as those described in the Materials and Methods section. A Group×Time×Mode ANOVA on estimates of modularity indicated greater overall modularity in younger than older adults (Group: $F_{1,36}$=25.06, p<0.001, η_p^2=0.41), greater modularity during resting-state than task mode (Mode: $F_{1.36}$=132.59, p<0.001, η_p^2=0.79), and greater decrement in modularity when switching from resting-state to task mode, in older compared to younger adults (Group×Mode: $F_{1,36}$=10.63, p=0.002, η_p^2=0.23) (Fig. S1a). Similarly, a Group×Time×Load ANOVA on estimates of modularity (loads 5-8) indicated greater overall modularity in younger than older adults (Group: $F_{1,36}$=38.26, p<0.001, η_p^2=0.52), a main effect of Load ($F_{3,108}$=4.16, p=0.013, ε=0.83, η_p^2=0.1), qualified by a significant linear trend ($F_{1,36}$=6.26, p=0.017, η_p^2=0.15), and a trending Group×Time interaction ($F_{2,72}$=2.92, p=0.06, η_p^2=0.08) (Fig. S1b). Separately assessing *task-exposure* (Time1 vs. Time2) and *training* effects (Time2 vs. Time3) between groups showed greater modularity in younger compared to older adults (ps<0.001) and a

significant Group×Time interaction with training ($F_{1,36}$=5.16, p=0.029, η_p^2=0.13) but not with task-exposure (p=0.3), indicating a greater effect of WM training on brain-wide modularity for younger compared to older adults. Within groups, older adults showed no task-exposure or training effects on modularity (ps>0.3), whereas younger adults showed greater modularity post- compared to pre-training (Time: $F_{1,19}$=13.07, p=0.002, η_p^2=0.41). In sum, we replicated our main results using different values of the Louvain resolution parameter, as well as a different brain atlas, confirming that results are robust and likely independent of particular analysis settings.

Consensus Partitions. We also repeated the consensus clustering analysis (set parameter γ = 1.3 for the Louvain algorithm) using different values for the thresholding parameter that covered a range of commonly employed values, τ = [0.3, 0.4, 0.5], and the results were similar. For all tau values, we identified similar major modules during resting-state, broadly corresponding to the visual, sensorimotor, salience/cingulo-opercular, fronto-parietal, and default-mode networks. In addition, we observed the same tendencies for both groups when switching from rest to task performance. Specifically, for older adults, a salience/sensorimotor module emerged when switching from rest to task modes, and for younger adults, the conjoined fronto-parietal/salience module emerged with increased WM load. Unsurprisingly, module separation (across time and loads) was relatively less consistent for τ = 0.3, whereas the number of singletons (i.e., communities composed of a single node) increased for τ = 0.5. Similar to other analyses presented above, these results confirm that that the observed differences in community structure are robust.

Pairwise Connectivity Analyses. Finally, to ensure that results were not due to a specific threshold value for pairwise connectivity, we repeated the analyses using a range of thresholds, p

= [0.005, 0.004, 0.003, 0.002, 0.001], and the results were broadly similar (see Tables S2 and S3).

Control Analyses

Spatial Smoothing. Because the main concern with using unsmoothed data is that misalignment of functional regions between older and younger adults may inflate group differences between participants (Geerligs et al., 2017), we ran a control analysis using a smoothing kernel of twice the voxel size (i.e., 6 mm). Modularity values were not additionally normalized to mitigate the effect of smoothing on null networks' properties. We again identified lower modularity for older than younger adults across all time points, for both the rest/task shift (Group: $F_{1,36}$=17.11, p<0.001, η_p^2=0.32) and across WM loads common to both groups (i.e., loads 5-8) (Group: $F_{1,36}$=33.62, p<0.001, η_p^2=0.48), as well as greater decrement in modularity with shifting from rest to task in older than younger adults (Group×Mode: $F_{1,36}$=17.14, p<0.001, η_p^2=0.32). These results indicate that the initial group differences in modularity are meaningful, and not simply an artifact of normalization inaccuracies. Of note, in our study we also took a number of additional measures to limit potential misalignment between participants: (1) we used Diffeomorphic Anatomical Registration Through Exponentiated Lie Algebra (DARTEL) (Ashburner, 2007), which is one of the best performing inter-participant registration and normalization approaches, recommended for both healthy and special/clinical populations (Bergouignan et al., 2009; Cuingnet et al., 2011; Klein et al., 2009; Yassa & Stark, 2009; Youssofzadeh et al., 2017); (2) we used a brain parcellation (i.e., Power et al., 2011) shown to provide superior homogeneity across younger and older participants (Geerligs et al., 2017) and successfully replicated our results using a different parcellation (Schaefer et al., 2018); and (3) we used 5 mm radius ROIs with a

practical outcome of employing a smoothing level proportional to the size of the ROIs (Triana et al., 2020).

Graph thresholding. We checked our density thresholding cutoffs (i.e., 10% – 30% of the strongest connections) and they satisfied all the criteria mentioned by Chong et al. (2019). Specifically, (1) the average number of edges per node varied in the range from 22 to 66 and was larger than the log of the total number of edges, which varied in the range from 7.8 to 8.89; (2) 99.3% and 98.5% of the nodes were fully connected in older and younger adults, respectively (thus, all >80%), for the most stringent threshold (i.e., 10% connection density); (3) small worldness of the network varied in the range from 2.41 to 1.4 in older adults, and in the range from 2.83 to 1.5 in younger adults (thus, all >1).

Mean connectivity regression and high-pass filtering. First, we checked whether regression of mean connectivity would influence between-group differences in modularity (Geerligs et al., 2017). For each pair of ROIs, we regressed mean connectivity strength—calculated as the mean connectivity strength across all connections in the unthresholded connectivity matrix, including absolute values of positive and negative values (Malagurski et al., 2020), and then averaged across all conditions—against the connectivity estimates of that pair, and retained the residuals. Similar to the results using modularity normalization (see main text), we identified lower modularity for older than younger adults across all time points, for both the rest/task shift (Group: $F_{1,36}$=13.88, p=0.001, η_p^2=0.28) and across WM loads common to both groups (i.e., loads 5-8) (Group: $F_{1,36}$=7.52, p=0.009, η_p^2=0.17), suggesting that differences in modularity between older and younger adults were not driven by group differences in mean connectivity. Second, we checked whether applying a high-pass filter (>0.01 Hz) instead of the band-pass filter (0.01–0.15 Hz) would influence the observed age effects. We similarly identified lower

modularity for older than younger adults across all time points, for both the rest/task shift (Group: $F_{1,36}$=13.56, p=0.001, η_p^2=0.27) and across WM loads common to both groups (i.e., loads 5-8) (Group: $F_{1,36}$=6.09, p=0.018, η_p^2=0.15).

Resting-state and task durations. The scan period for resting-state (duration = 470 s) was longer than the concatenated time series for each of the working memory conditions (duration = 168 s, for each WM load). To check if differences in scanning time might account for differences between rest and task modes, we equated the duration of resting-state and WM conditions by focusing on the last 168 seconds of the resting-state series. The results were similar to our initial analysis. Specifically, a Group×Time×Mode ANOVA on estimates of modularity indicated greater modularity during resting-state than task mode ($F_{1,36}$=62.89, p<0.001, η_p^2=0.64) and greater decrement in modularity when switching from resting-state to task mode, in older compared to younger adults (Group×Mode: $F_{1,36}$=13.63, p=0.001, η_p^2=0.28) (see Fig. S5).

Finite Impulse Response (FIR) task regression. To test whether our HRF-based task regression accounted effectively for task-evoked activations (Cole et al., 2019), we performed a control analysis using FIR task regression. Specifically, we fit a series of 10 regressors, one per time point, separately for encoding and retrieval, covering a time window of 20 s, to account for the likely duration of the HRF. Of note, it was not feasible to model separate FIRs also by condition (120 regressors total) given the length of our time series (168 TRs per run), because the connectivity measures would become too noisy to be useful (i.e., very low [~10] estimated remaining degrees of freedom and very high variability of the diagnostic voxel-to-voxel correlational histograms); this is a known limitation of FIR (Poline & Brett, 2012). Nevertheless, FIR task regression provided results similar to our initial approach employing HRF task regression. Specifically, we identified lower modularity for older than younger adults across all

time points, for both the rest/task shift (Group: $F_{1,36}$=23.7, p<0.001, η_p^2=0.4) and across WM loads common to both groups (i.e., loads 5-8) (Group: $F_{1,36}$=24.01, p<0.001, η_p^2=0.4), as well as greater modularity decrement with shifting from rest to task mode in older compared to younger adults (Group×Mode: $F_{1,36}$=6.82, p=0.013, η_p^2=0.16). Critically, we confirmed a Group×Time interaction with training (i.e., Time2 vs. Time3) (Group×Time: $F_{1,36}$=4.8, p=0.035, η_p^2=0.12), indicating increased modularity with training in younger than older adults. Finally, within groups and across group-specific loads (i.e., loads 5-9 in younger adults and 4-8 in older adults), younger adults showed increased modularity with training (Time: $F_{1,19}$=10.89, p=0.004, η_p^2=0.36), whereas older adults showed no training effects on modularity (Time: $F_{1,17}$=0.38, p=0.55, η_p^2=0.02). Thus, the consistent results across both types of task regression (i.e., HRF and FIR-based) suggest that HRF-based task regression can effectively account for task-evoked activations, at least for a Sternberg-like working memory task, when the analyses focus on the maintenance interval.

Table S1. Robustness analysis results for whole-brain modularity effects.

Analysis & Effects	Statistic	Gamma				
		1.0	1.1	1.2	1.3	1.4
Rest-to-task shift: Group×Time×Mode ANOVA						
Group	$F_{1,36}$	32.46 (<0.001)	32.49 (<0.001)	32.57 (<0.001)	31.99 (<0.001)	31.13 (<0.001)
Mode	$F_{1,36}$	134.93 (<0.001)	130.21 (<0.001)	133.63 (<0.001)	141.51 (<0.001)	149.94 (<0.001)
Group×Mode	$F_{1,36}$	14.08 (0.001)	15.82 (<0.001)	17.48 (<0.001)	19.14 (<0.001)	20.63 (<0.001)
Working memory load: Group×Time×Load ANOVA						
Group	$F_{1,36}$	34.17 (<0.001)	35.68 (<0.001)	36.2 (<0.001)	37.38 (<0.001)	38.38 (<0.001)
Time	$F_{2,72}$	N.S.	N.S.	N.S.	N.S.	N.S.
Load	$F_{3,108}$	3.96 (0.015)	4.27 (0.007)	4.94 (0.003)	5.89 (0.001)	6.9 (<0.001)
Linear trend	$F_{1,36}$	7.82 (0.008)	8.74 (0.005)	10.56 (0.003)	13.52 (0.001)	17.09 (<0.001)
Group×Load	$F_{3,108}$	3.28 (0.024)	3.42 (0.02)	3.42 (0.02)	3.21 (0.026)	2.86 (0.04)
Group×Time	$F_{2,72}$	4.85 (0.011)	4.92 (0.01)	4.79 (0.011)	4.64 (0.013)	4.4 (0.016)

Table S1. Continued.

Analysis & Effects	Statistic	Gamma					
		1.5	1.6	1.7	1.8	1.9	2.0
Rest-to-task shift: Group×Time×Mode ANOVA							
Group	$F_{1,36}$	30.57 (<0.001)	30.04 (<0.001)	29.81 (<0.001)	29.79 (<0.001)	29.72 (<0.001)	29.39 (<0.001)
Mode	$F_{1,36}$	158.49 (<0.001)	168.58 (<0.001)	176.67 (<0.001)	181.34 (<0.001)	181.47 (<0.001)	178.39 (<0.001)
Group×Mode	$F_{1,36}$	22 (<0.001)	23.11 (<0.001)	24.27 (<0.001)	25.4 (<0.001)	25.87 (<0.001)	25.9 (<0.001)
Working memory load: Group×Time×Load ANOVA							
Group	$F_{1,36}$	39.4 (<0.001)	40.39 (<0.001)	41.25 (<0.001)	42.12 (<0.001)	43.09 (<0.001)	43.82 (<0.001)
Time	$F_{2,72}$	3.35 (0.041)	3.89 (0.025)	4.51 (0.013)	5.28 (0.007)	6.19 (0.003)	7.22 (0.001)
Load	$F_{3,108}$	7.78 (<0.001)	8.59 (<0.001)	9.08 (<0.001)	9.52 (<0.001)	9.9 (<0.001)	10.18 (<0.001)
Linear trend	$F_{1,36}$	20.89 (<0.001)	25.28 (<0.001)	27.75 (<0.001)	30.68 (<0.001)	33.44 (<0.001)	35.64 (<0.001)
Group×Load	$F_{3,108}$	N.S.	N.S.	N.S.	N.S.	N.S.	N.S.
Group×Time	$F_{2,72}$	4.19 (0.019)	4.01 (0.022)	3.82 (0.026)	3.64 (0.031)	3.45 (0.037)	3.25 (0.044)

Table S2. Robustness analysis for pairwise connectivity for older adults.

Threshold		$t = 2.9$, $p = 0.005$	$t = 3$, $p = 0.004$	$t = 3.14$, $p = 0.003$	$t = 3.33$, $p = 0.002$	$t = 3.65$, $p = 0.001$
Contrast						
Training:	*Time3 > Time2*					
	N networks	1	1	1	1	N.S.
	P-value	0.028	0.038	0.043	0.045	
	N edges	232	180	122	55	
	N nodes	173	147	110	52	
Load:	*High > Low*					
	N networks	1	1	1	1	1
	P-value	<0.001	<0.001	<0.001	<0.001	<0.001
	N edges	380	335	266	191	103
	N nodes	162	156	137	112	81
	Low > High					
	N networks	1	1	1	1	1
	P-value	0.019	0.016	0.014	0.023	0.012
	N edges	207	165	123	52	22
	N nodes	139	120	99	45	21

Note: P-values are family-wise error corrected at the network level.

Table S3. Robustness analysis for pairwise connectivity for younger adults.

Threshold		$t = 2.86$, $p = 0.005$	$t = 2.96$, $p = 0.004$	$t = 3.09$, $p = 0.003$	$t = 3.27$, $p = 0.002$	$t = 3.58$, $p = 0.001$	
Contrast							
Training:	*Time2 > Time3*						
	N networks	1	1	1	1		2
	P-value	0.003	0.002	0.001	0.001	0.004	0.032
	N edges	283	235	182	120	40	19
	N nodes	166	150	128	97	41	16
Load:	*High > Low*						
	N networks	1	1	1	1		1
	P-value	0.046	0.031	0.03	0.021		0.032
	N edges	179	147	108	64		19
	N nodes	125	106	89	58		20
	Low > High						
	N networks	1	1	1	1		1
	P-value	<0.001	0.001	<0.001	0.001		0.004
	N edges	284	228	181	106		37
	N nodes	160	146	131	90		35

Note: P-values are family-wise error corrected at the network level.

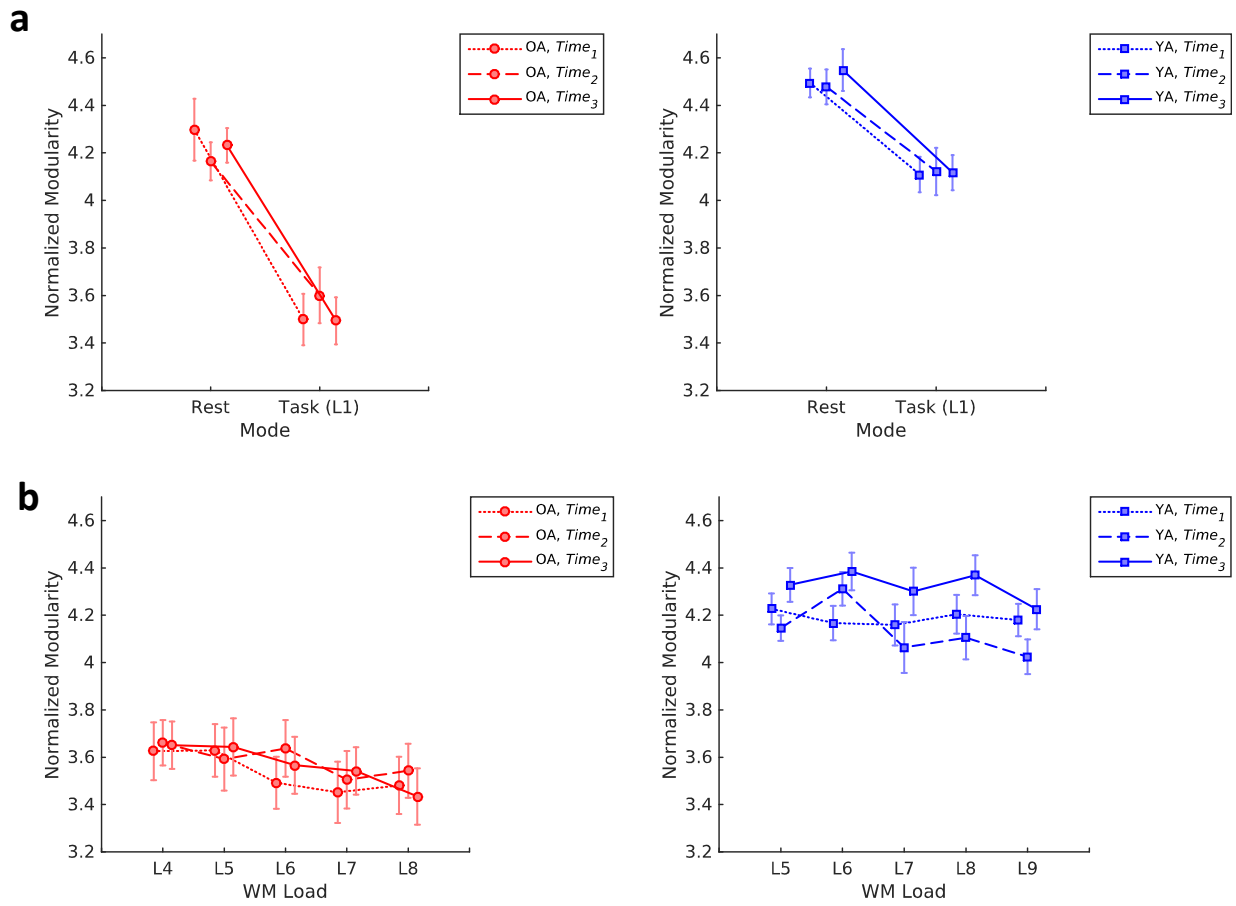

Fig. S1. Robustness analysis for effects on brain-wide modularity, using the Schaefer et al. (2018) atlas. a, Effect of switching between resting-state and task mode (i.e., load of 1) on modularity. **b**, Effect of WM load on modularity. Results were overall similar to those obtained using the Power et al. (2011) atlas. Errorbars show standard error of the mean. OA, older adults; YA, younger adults; WM, working memory.

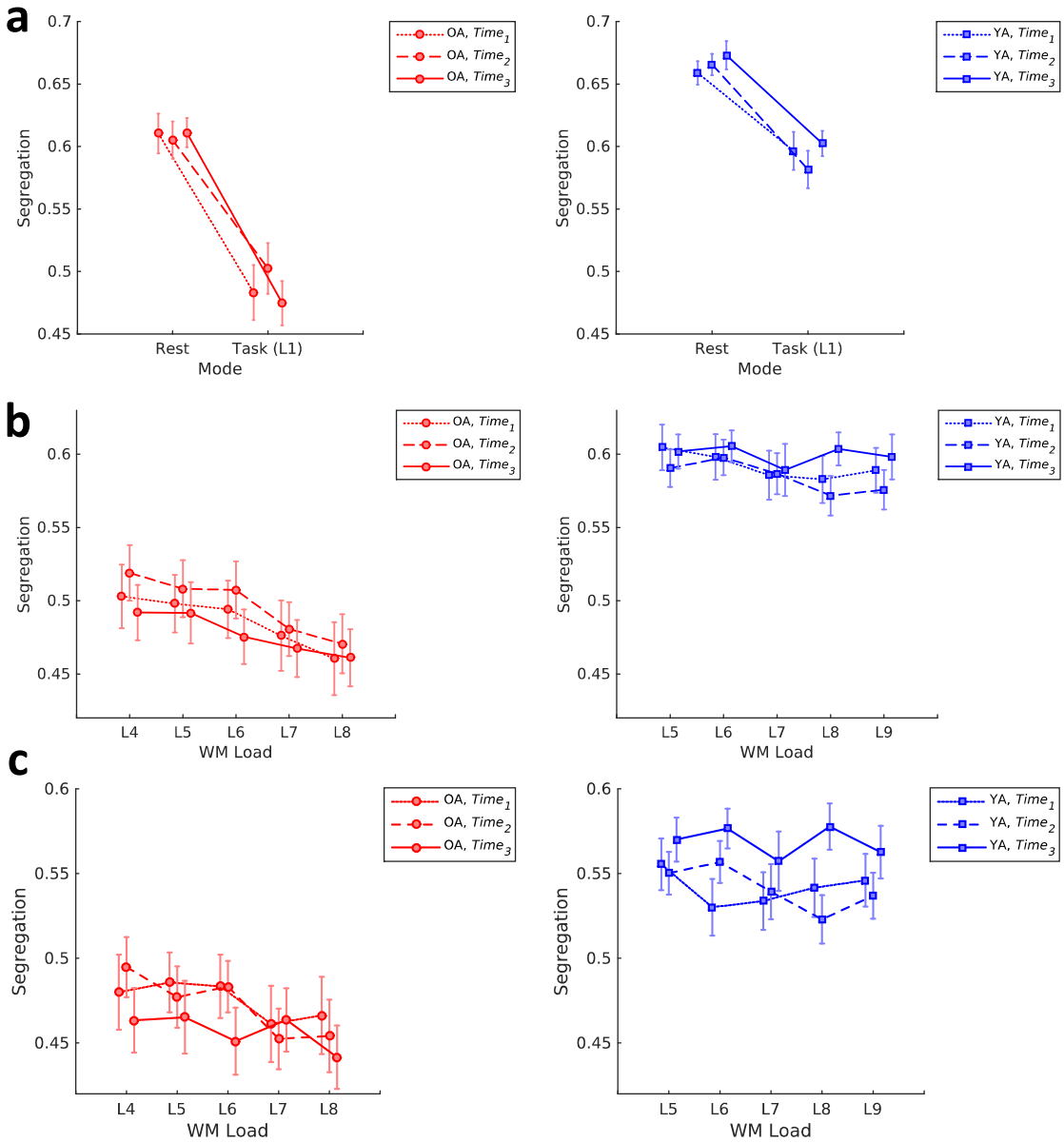

Fig. S2. Network segregation calculated using the canonical (i.e., resting-state) networks versus data-driven networks. Effects of **(a)** switching between resting-state and task mode (i.e., load of 1) and **(b)** WM load on segregation calculated using the Power et al. (2011) canonical networks. Results were overall similar to those obtained using the modularity metric, but the effects of training were relatively less specific. However, when segregation was calculated using the data-driven community structure detected for each individual condition **(c)**, younger adults showed greater segregation with training whereas older adults did not, consistent with our modularity results. Error bars display standard error of the mean. OA, older adults; YA, younger adults; WM, working memory.

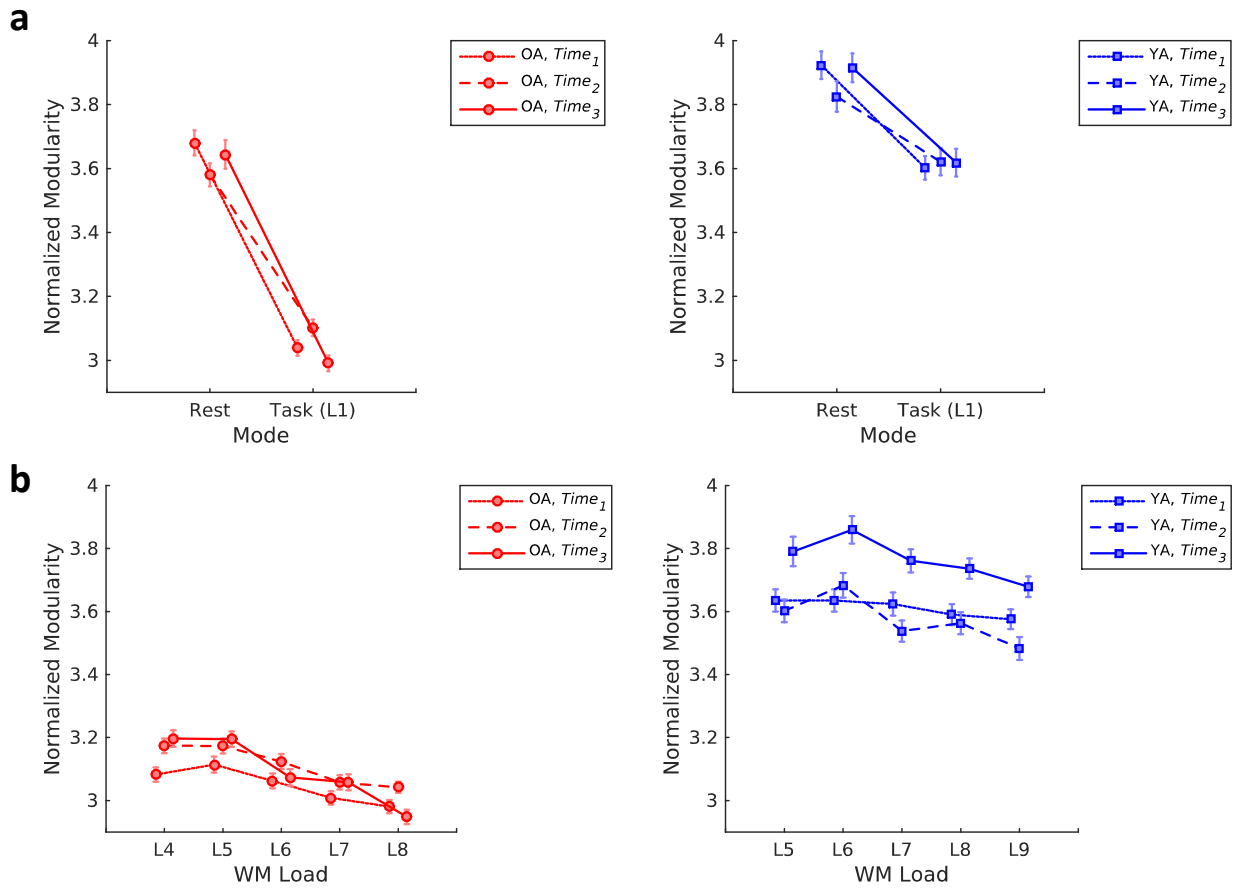

Fig. S3. Normalized modularity across gamma range. Line graphs display mean normalized modularity calculated across gamma values between 1 and 2 in increments of 0.1. Error bars display standard error of the mean. OA, older adults; YA, younger adults; WM, working memory.

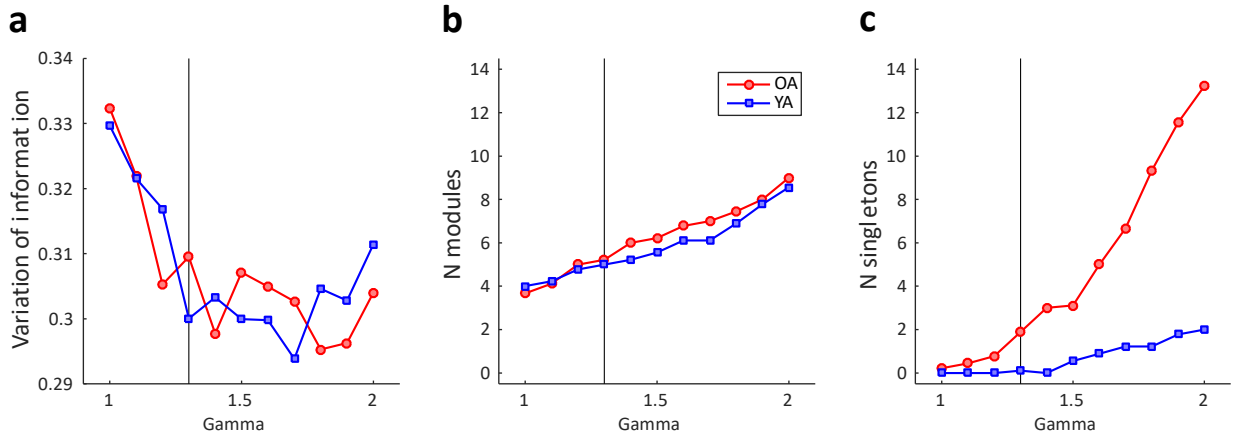

Fig. S4. Variation of information relative to the Power et al. networks (a), number of modules (b), and number of singletons (c). Values are displayed for group-level partitions at different levels of gamma, for older (OA) and younger adults (YA). Vertical line identifies gamma = 1.3. Error bars are not drawn because line graphs are based on group-level partitions.

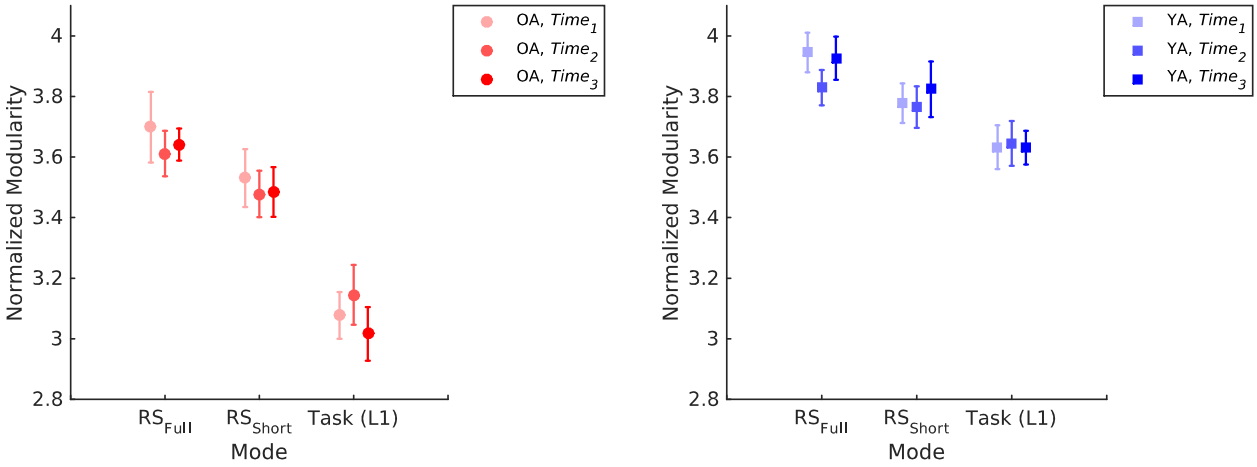

Fig. S5. Normalized modularity calculated for full (RS_{Full}) and shorter resting-state (RS_{Short}) period, equal with the duration of WM conditions. The relevant comparison is between RS_{Short} and Task (Load of 1). Errorbars display standard error of the mean. OA, older adults; YA, younger adults.

References

Ashburner, J. (2007). A fast diffeomorphic image registration algorithm. *Neuroimage, 38*(1), 95-113. doi:10.1016/j.neuroimage.2007.07.007

Bergouignan, L., Chupin, M., Czechowska, Y., Kinkingnéhun, S., Lemogne, C., Le Bastard, G., . . . Fossati, P. (2009). Can voxel based morphometry, manual segmentation and automated segmentation equally detect hippocampal volume differences in acute depression? *Neuroimage, 45*(1), 29-37. doi:https://doi.org/10.1016/j.neuroimage.2008.11.006

Chan, M. Y., Park, D. C., Savalia, N. K., Petersen, S. E., & Wig, G. S. (2014). Decreased segregation of brain systems across the healthy adult lifespan. *Proc Natl Acad Sci U S A, 111*(46), E4997-5006. doi:10.1073/pnas.1415122111

Chong, J. S. X., Ng, K. K., Tandi, J., Wang, C., Poh, J.-H., Lo, J. C., . . . Zhou, J. H. (2019). Longitudinal Changes in the Cerebral Cortex Functional Organization of Healthy Elderly. *The Journal of Neuroscience, 39*(28), 5534. doi:10.1523/JNEUROSCI.1451-18.2019

Cole, M. W., Ito, T., Schultz, D., Mill, R., Chen, R., & Cocuzza, C. (2019). Task activations produce spurious but systematic inflation of task functional connectivity estimates. *Neuroimage, 189*, 1-18. doi:10.1016/j.neuroimage.2018.12.054

Cuingnet, R., Gerardin, E., Tessieras, J., Auzias, G., Lehéricy, S., Habert, M. O., . . . Colliot, O. (2011). Automatic classification of patients with Alzheimer's disease from structural MRI: a comparison of ten methods using the ADNI database. *Neuroimage, 56*(2), 766-781. doi:10.1016/j.neuroimage.2010.06.013

Geerligs, L., Tsvetanov, K. A., & Henson, R. N. (2017). Challenges in measuring individual differences in functional connectivity using fMRI: The case of healthy aging. *Hum Brain Mapp, 38*(8), 4125-4156. doi:10.1002/hbm.23653

Hughes, C., Faskowitz, J., Cassidy, B. S., Sporns, O., & Krendl, A. C. (2020). Aging relates to a disproportionately weaker functional architecture of brain networks during rest and task states. *Neuroimage, 209*, 116521. doi:10.1016/j.neuroimage.2020.116521

Klein, A., Andersson, J., Ardekani, B. A., Ashburner, J., Avants, B., Chiang, M. C., . . . Parsey, R. V. (2009). Evaluation of 14 nonlinear deformation algorithms applied to human brain MRI registration. *Neuroimage, 46*(3), 786-802. doi:10.1016/j.neuroimage.2008.12.037

Malagurski, B., Liem, F., Oschwald, J., Mérillat, S., & Jäncke, L. (2020). Functional dedifferentiation of associative resting state networks in older adults – A longitudinal study. *Neuroimage*, 116680. doi:https://doi.org/10.1016/j.neuroimage.2020.116680

Meilă, M. (2007). Comparing clusterings—an information based distance. *Journal of Multivariate Analysis, 98*(5), 873-895. doi:https://doi.org/10.1016/j.jmva.2006.11.013

Poline, J. B., & Brett, M. (2012). The general linear model and fMRI: does love last forever? *Neuroimage, 62*(2), 871-880. doi:10.1016/j.neuroimage.2012.01.133

Power, J. D., Cohen, A. L., Nelson, S. M., Wig, G. S., Barnes, K. A., Church, J. A., . . . Petersen, S. E. (2011). Functional network organization of the human brain. *Neuron, 72*(4), 665-678. doi:10.1016/j.neuron.2011.09.006

Schaefer, A., Kong, R., Gordon, E. M., Laumann, T. O., Zuo, X. N., Holmes, A. J., . . . Yeo, B. T. T. (2018). Local-Global Parcellation of the Human Cerebral Cortex from Intrinsic Functional Connectivity MRI. *Cereb Cortex, 28*(9), 3095-3114. doi:10.1093/cercor/bhx179

Triana, A. M., Glerean, E., Saramäki, J., & Korhonen, O. (2020). Effects of spatial smoothing on group-level differences in functional brain networks. *Network Neuroscience, 4*(3), 556-574. doi:10.1162/netn_a_00132

Wig, G. S. (2017). Segregated Systems of Human Brain Networks. *Trends Cogn Sci, 21*(12), 981-996. doi:10.1016/j.tics.2017.09.006

Yassa, M. A., & Stark, C. E. (2009). A quantitative evaluation of cross-participant registration techniques for MRI studies of the medial temporal lobe. *Neuroimage, 44*(2), 319-327. doi:10.1016/j.neuroimage.2008.09.016

Youssofzadeh, V., McGuinness, B., Maguire, L. P., & Wong-Lin, K. (2017). Multi-Kernel Learning with Dartel Improves Combined MRI-PET Classification of Alzheimer's Disease in AIBL Data: Group and Individual Analyses. *11*(380). doi:10.3389/fnhum.2017.00380